САМАРСКИЙ УНИВЕРСИТЕТ
SAMARA UNIVERSITY

Methods and Algorithms for Nanosatellite Attitude Determination

Dr. Petr Nikolaev

Samara 2021

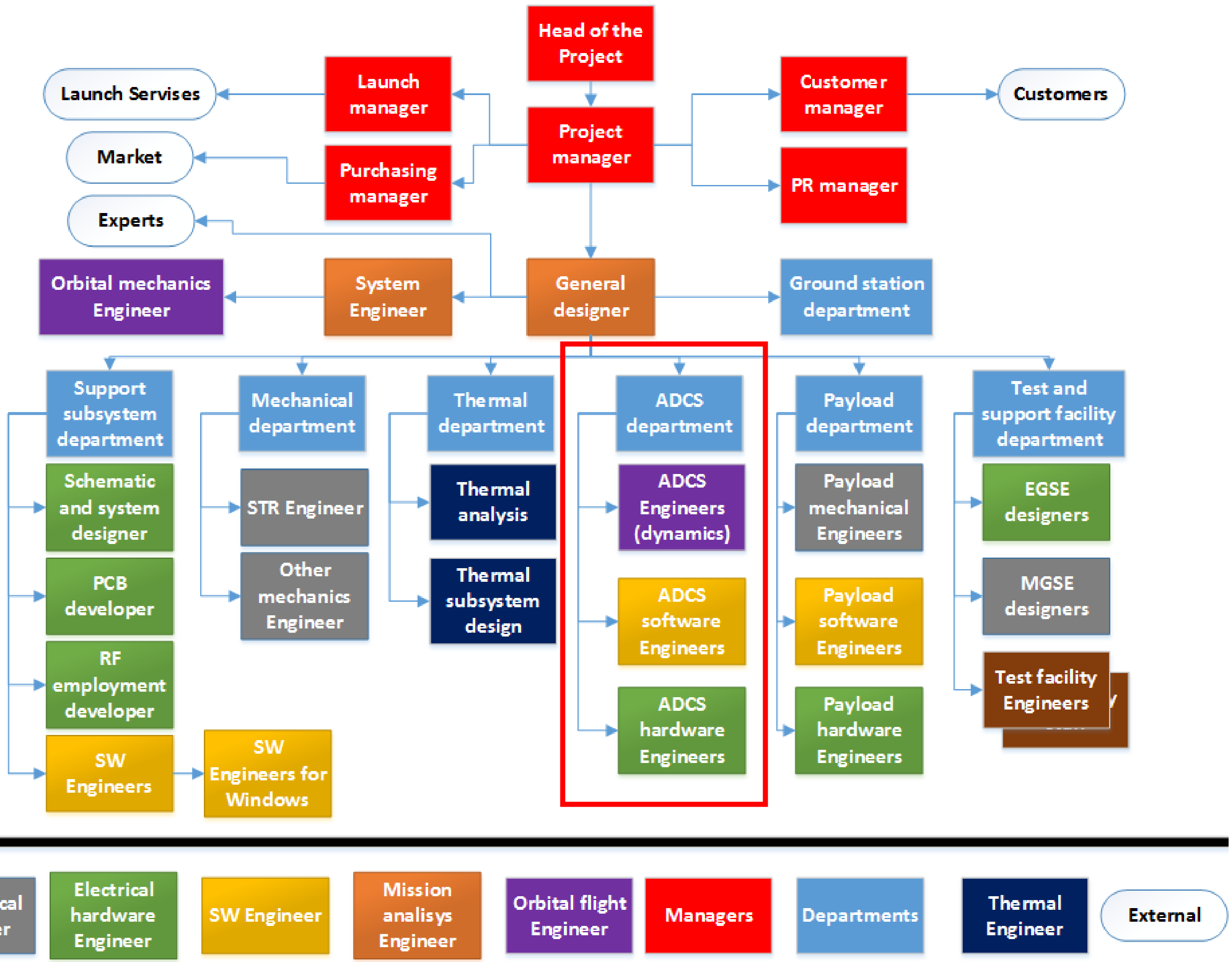
Head of the Project
Project manager
Launch manager
Purchasing manager
Customer manager
PR manager
Launch Servises
Market
Experts
Customers
General designer
System Engineer
Orbital mechanics Engineer
Ground station department
Support subsystem department
Schematic and system designer
PCB developer
RF employment developer
SW Engineers
SW Engineers for Windows
Mechanical department
STR Engineer
Other mechanics Engineer
Thermal department
Thermal analysis
Thermal subsystem design
ADCS department
ADCS Engineers (dynamics)
ADCS software Engineers
ADCS hardware Engineers
Payload department
Payload mechanical Engineers
Payload software Engineers
Payload hardware Engineers
Test and support facility department
EGSE designers
MGSE designers
Test facility Engineers
Mechanical Engineer
Electrical hardware Engineer
SW Engineer
Mission analisys Engineer
Orbital flight Engineer
Managers
Departments
Thermal Engineer
External

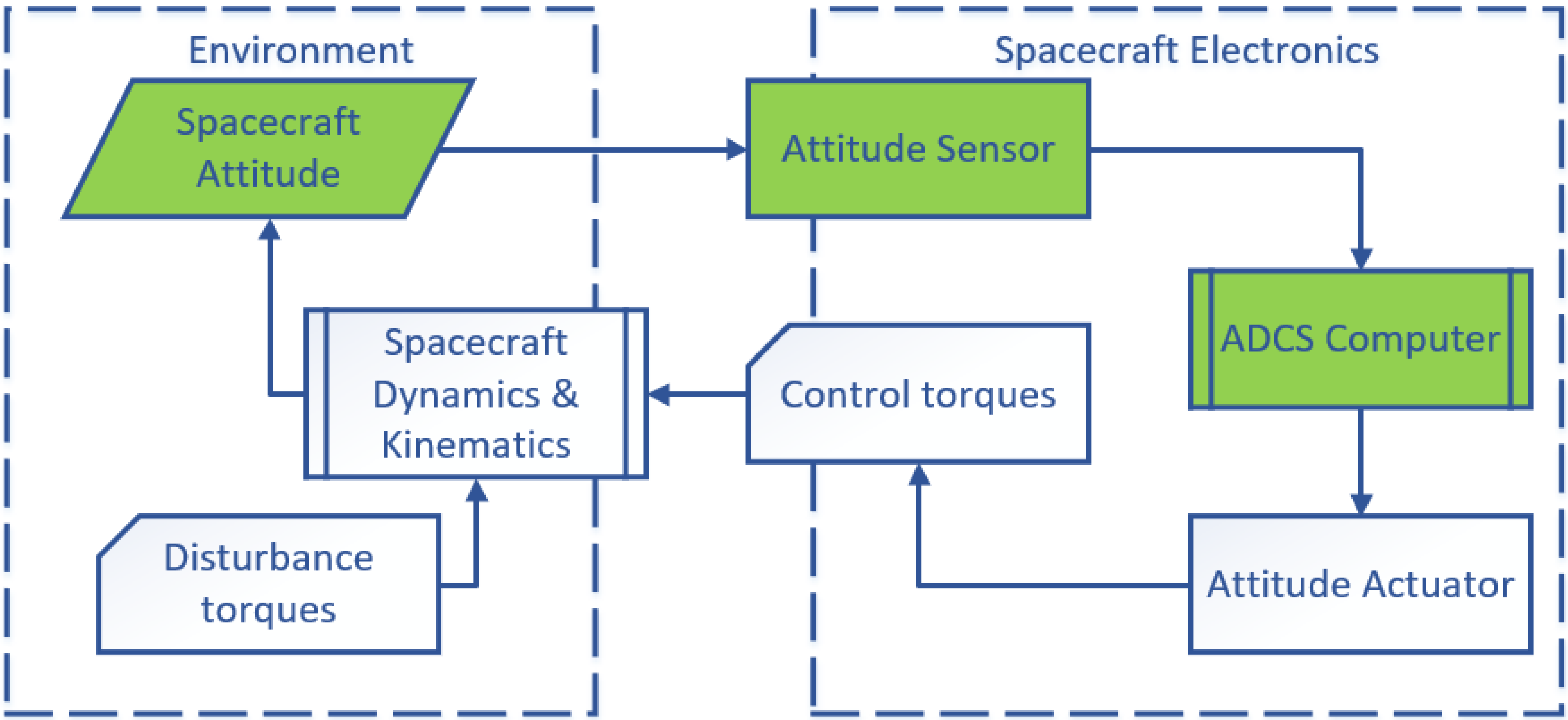

ADCS closed-loop control system

The main frames of reference:

- the **body frame** of reference (BFR)
- the **orbital frame** of reference (OFR);
- the **geocentric frame** of reference (GFR).

Attitude matrix:

$$M_{X_1X_2} = \begin{cases} f_1(\vartheta, \psi, \varphi), \\ f_2(q_0, q_1, q_2, q_3), \\ f_3(m_{ij}, \quad i,j = \overline{1,3}). \end{cases}$$

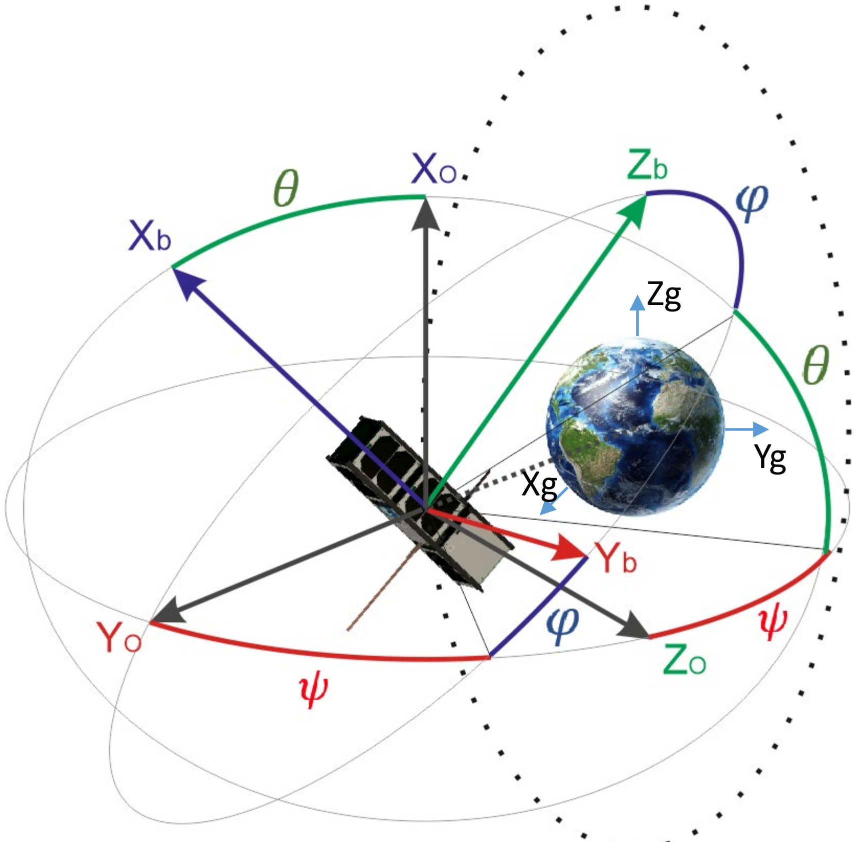

Fig. 1.1 – The frames of reference

$$\mathbf{M}_{X_1X_2} = [m_{ij}]_{i,j=\overline{1,3}} = \begin{bmatrix} \cos\vartheta\cdot\cos\psi & \cos\vartheta\cdot\sin\psi & -\sin\vartheta \\ \sin\varphi\cdot\sin\vartheta\cdot\cos\psi - \cos\varphi\cdot\sin\psi & \sin\varphi\cdot\sin\vartheta\cdot\sin\psi + \cos\varphi\cdot\cos\psi & \sin\varphi\cos\vartheta \\ \cos\varphi\cdot\sin\vartheta\cdot\cos\psi + \sin\varphi\cdot\sin\psi & \cos\varphi\cdot\sin\vartheta\cdot\sin\psi - \sin\varphi\cdot\cos\psi & \cos\varphi\cos\vartheta \end{bmatrix}$$

Moskovskoye shosse, 34, Samara, 443086, Russia, tel.: +7 (846) 335-18-26, fax: +7 (846) 335-18-36, www.ssau.ru, e-mail: ssau@ssau.ru

Representation of Attitude

Representation	Par.	Characteristic	Application
Rotation matrix	9	• Inherently nonsingular • Intuitive representation • Difficult to mantain ortogonality • Expensive to store • Six redundant parameter	Analytical studies and transformation of vectors.
Euler angles	3	• Minimal set • Clear physical interpretation • Trigometric functions in rotation matrix • No simple composition rule • Singular for certain rotations • Trigonometric functions in kinematic relation	Theoretical physics, spinning spacecraft and attitude maneuvers. Used in analytical studies.
Axis-azimuth	3	• Minimal set • Clear physical interpretation • Often computed directly from observations • No simple composition rule • Computation of rotating matrix very difficult • Singular for certain rotation • Trigonometric functions in kinematic relation	Primarily spinning spacecraft.
Rodriguez (Gibbs)	3	• Minimal set • Clear physical interpretation • Singular for rotations near $\theta = \pm\pi$ • Simple kinematic relations	Often interpreted as incremental rotation vector.
Quaternions	4	• Easy orthogonality of rotation matrix • Bilinear composition rule • Not singular at any rotation matrix • Linear kinematic equations • No clear physical interpretation • One redundant parameter • Simple kinematic relation	Widely used in smulations and data processing. Preferred attitude representation for attitude control systems.

Moskovskoye shosse, 34, Samara, 443086, Russia, tel.: +7 (846) 335-18-26, fax: +7 (846) 335-18-36, www.ssau.ru, e-mail: ssau@ssau.ru

Rotation matrix depending on the Euler angles

$$A_{yzy} = \begin{bmatrix} \cos\varphi\cos\alpha\cos\psi - \sin\varphi\sin\psi & \cos\varphi\sin\alpha & -\cos\varphi\cos\alpha\sin\psi - \sin\varphi\cos\psi \\ -\sin\alpha\cos\psi & \cos\alpha & \sin\alpha\sin\psi \\ \sin\varphi\cos\alpha\cos\psi + \cos\varphi\sin\psi & \sin\varphi\sin\alpha & -\sin\varphi\cos\alpha\sin\psi + \cos\varphi\cos\psi \end{bmatrix}$$

Rotation matrix depending on the quaternion

$$A = \begin{bmatrix} 1 - 2(q_2^2 + q_3^2) & 2(q_1 q_2 - q_3 q_0) & 2(q_1 q_3 + q_2 q_0) \\ 2(q_1 q_2 + q_3 q_0) & 1 - 2(q_1^2 + q_3^2) & 2(q_2 q_3 - q_1 q_0) \\ 2(q_1 q_3 - q_2 q_0) & 2(q_2 q_3 + q_1 q_0) & 1 - 2(q_1^2 + q_2^2) \end{bmatrix}$$

Quaternion depending on the Euler angles

$$q_0 = \cos\frac{\alpha}{2}\cos\frac{\psi+\varphi}{2}\ ;\ q_1 = \sin\frac{\alpha}{2}\sin\frac{\psi-\varphi}{2}\ ;\ q_3 = \cos\frac{\alpha}{2}\sin\frac{\psi+\varphi}{2}\ ;\ q_4 = \sin\frac{\alpha}{2}\cos\frac{\psi-\varphi}{2}$$

Moskovskoye shosse, 34, Samara, 443086, Russia, tel.: +7 (846) 335-18-26, fax: +7 (846) 335-18-36, www.ssau.ru, e-mail: ssau@ssau.ru

Two main categories of attitude sensors

Reference Sensors	Inertial Sensors
Sun Sensor	Gyroscope
Star Tracker	Accelerometer
Magnetometer	

1

2

3

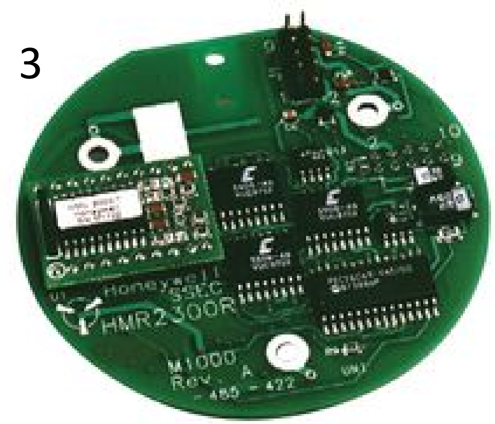

4

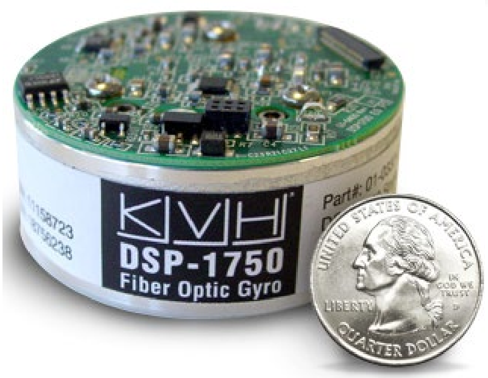

1. NanoSSOC-D60 Digital Sun Sensor
2. MAI-SS Space Sextant
3. HMR2300R-485 3-AXIS Magnetometer
4. DSP-1750 Optical Sensor (gyro)

MPU-9250 microchip

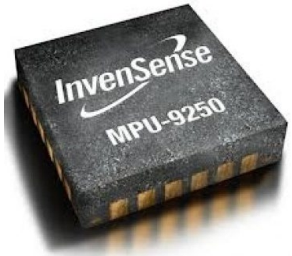

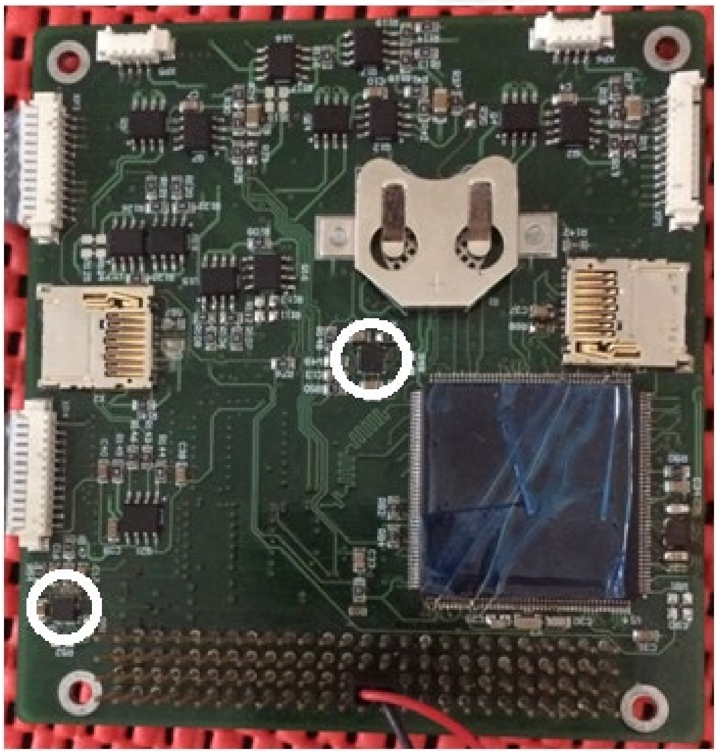

Location of MPU-9250 sensors on OBC of **SamSat** platform

Gyroscope

range of measuring ±250 °/s
sensitivity scale factor 131 LSB/(º/s)
digitally-programmable low-pass filter
total RMS Noise 0.1 º/s-rms
rate noise spectral density 0.01 º/s/√Hz
zero shift of the gyroscope measurements has a nonlinear temperature characteristic.

Magnetometer

range of measuring ± 4800μT
sensitivity scale factor 0.6μT/LSB
zero shift of the gyroscope measurements has a linear temperature characteristic.

MPU-9250 coordinate system

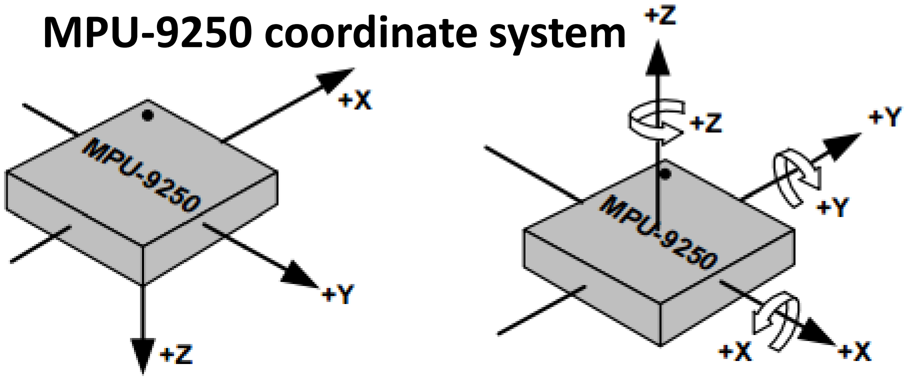

Magnetometer Accelerometer & Gyro

* https://www.invensense.com/wp-content/uploads/2015/02/PS-MPU-9250A-01-v1.1.pdf

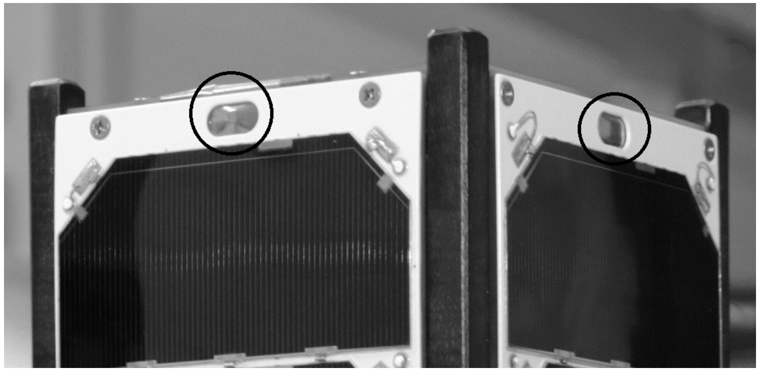

Location of light sensors on SamSat platform

TCS34725 Color (Sun) Sensor

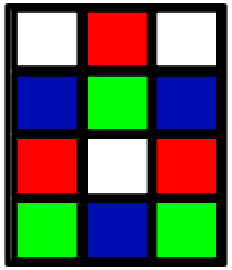

Red-filtered, green-filtered, blue-filtered, and clear (unfiltered) photodiodes

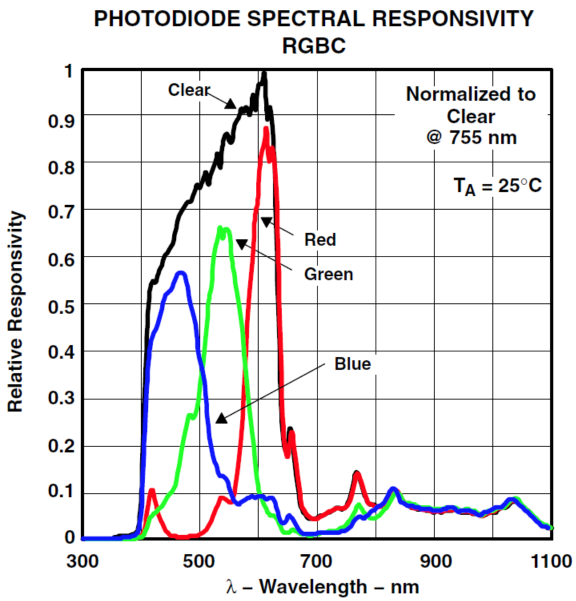

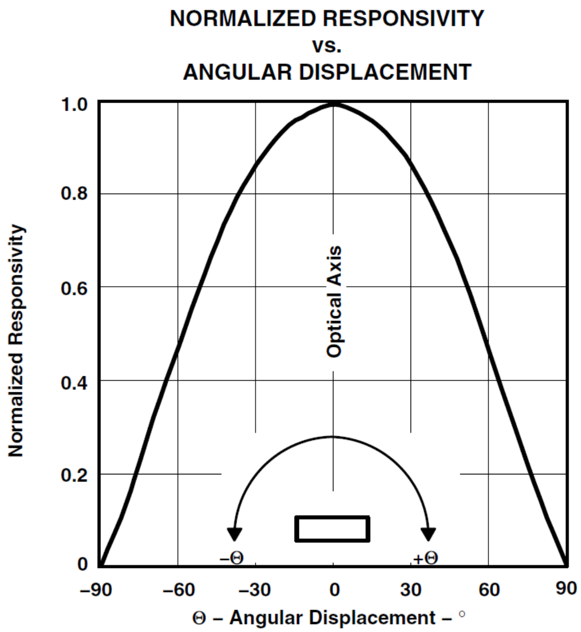

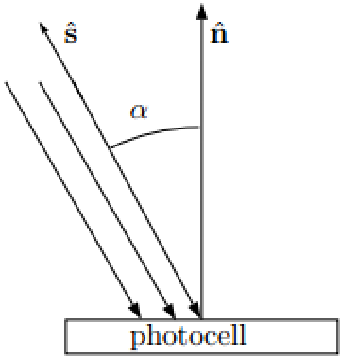

* https://cdn-shop.adafruit.com/datasheets/TCS34725.pdf

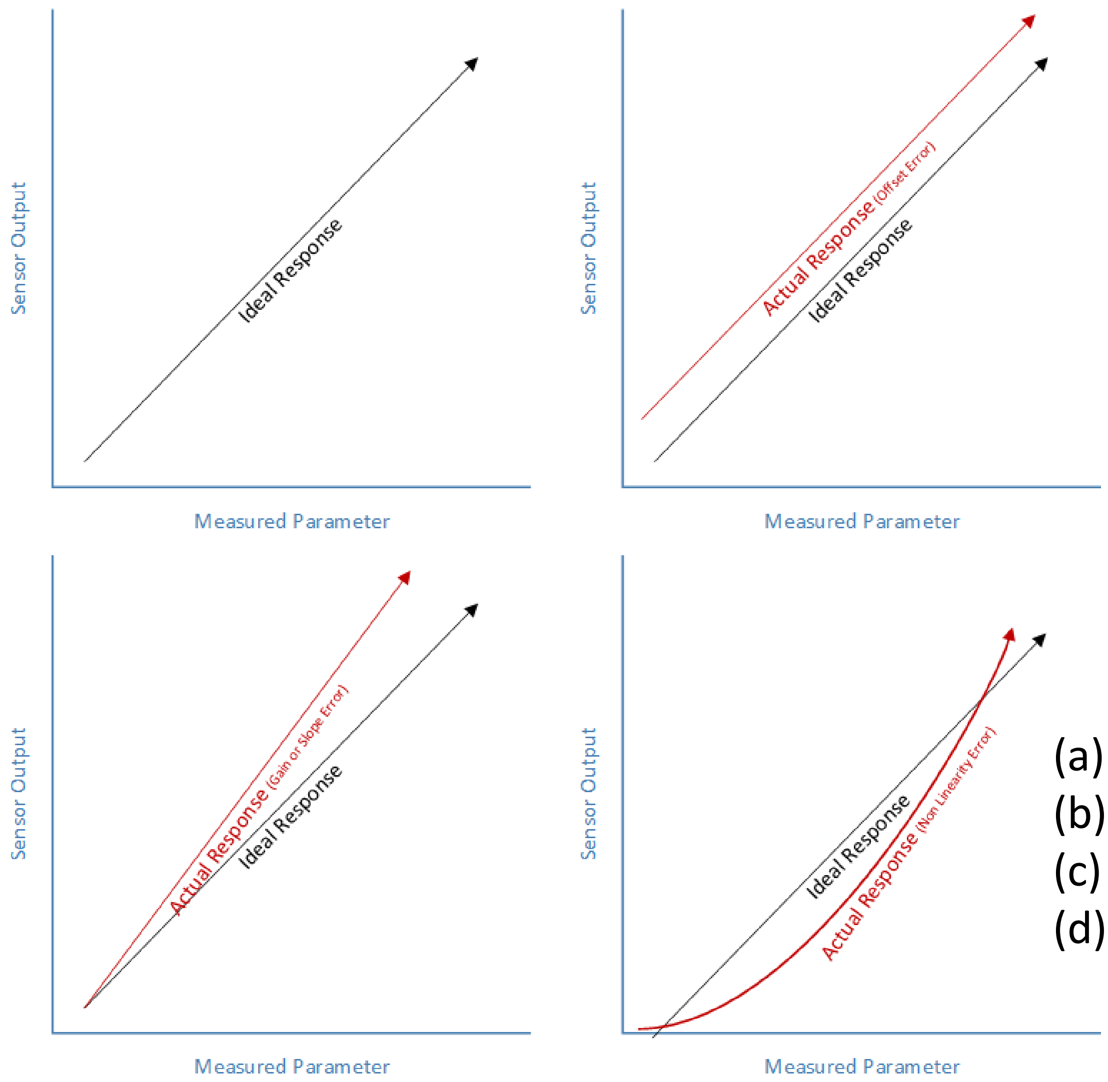

Types of errors:

- Bias;
- Scale factor;
- Nonlinearity;
- Noise;
- Depending from temperature etc.

(a) Ideal Response;
(b) Actual Response (bias error);
(c) Actual Response (scale factor error);
(d) Actual Response (non linearity error).

Example: **Calibrating the accelerometer**

$$\begin{bmatrix} A_{x1} \\ A_{y1} \\ A_{z1} \end{bmatrix} = [A\_m]_{3x3} \begin{bmatrix} 1/A\_SC_x & 0 & 0 \\ 0 & 1/A\_SC_y & 0 \\ 0 & 0 & 1/A\_SC_z \end{bmatrix} \cdot \begin{bmatrix} A_x - A\_OS_x \\ A_y - A\_OS_y \\ A_z - A\_OS_z \end{bmatrix}$$

$$= \begin{bmatrix} ACC_{11} & ACC_{12} & ACC_{13} \\ ACC_{21} & ACC_{22} & ACC_{23} \\ ACC_{31} & ACC_{32} & ACC_{33} \end{bmatrix} \cdot \begin{bmatrix} A_x \\ A_y \\ A_z \end{bmatrix} + \begin{bmatrix} ACC_{10} \\ ACC_{20} \\ ACC_{30} \end{bmatrix}$$

where [A_m] is the 3 x 3 **misalignment matrix** between the accelerometer sensing axes and the device body axes, A_SCi (i = x, y, z) is **the sensitivity (or scale factor)** and A_OSi is the zero-g level (or **offset**).

The goal of accelerometer calibration is to determine **12 parameters** from ACC_{10} to ACC_{33}, so that with any given raw measurements at arbitrary positions.

Example: Calibrating the accelerometer

Table 1. Sign definition of sensor raw measurements

Stationary position	Accelerometer (signed integer)		
	A_x	A_y	A_z
Z_b down	0	0	+1 *g*
Z_b up	0	0	-1 *g*
Y_b down	0	+1 *g*	0
Y_b up	0	-1 *g*	0
X_b down	+1 *g*	0	0
X_b up	-1 *g*	0	0

$$\begin{bmatrix} A_{x1} & A_{y1} & A_{z1} \end{bmatrix} = \begin{bmatrix} A_x & A_y & A_z & 1 \end{bmatrix} \cdot \begin{bmatrix} ACC_{11} & ACC_{21} & ACC_{31} \\ ACC_{12} & ACC_{22} & ACC_{32} \\ ACC_{13} & ACC_{23} & ACC_{33} \\ ACC_{10} & ACC_{20} & ACC_{30} \end{bmatrix}$$

or

$$Y = w \cdot X$$

where:

- Matrix **X** is the 12 calibration parameters that need to be determined
- Matrix **w** is sensor raw data LSBs collected at 6 stationary positions
- Matrix **Y** is the known normalized Earth gravity vector

Therefore, the calibration parameter matrix X can be determined by the **least square method** as:

$$X = \left[w^T \cdot w \right]^{-1} \cdot w^T \cdot Y$$

Attitude determination uses a combination of sensors and mathematical models to collect vector components in the body and inertial reference frames. These components are used in one of several different algorithms to determine the attitude, typically in the form of a quaternion, Euler angles, or a rotation matrix. It takes at least two vectors to estimate the attitude.

In general, the attitude determination solutions fall into two groups:
– **Deterministic (point-by-point)** solutions, where the attitude is found based on two or more vector observations from a single point in time,
– **Filters**, **recursive stochastic estimators** that statistically combine measurements from several sensors and often dynamic and/or kinematic models in order to achieve an estimate of the attitude.

34, Moskovskoye shosse, Samara, 443086, Russia, tel.: +7 (846) 335-18-26, fax: +7 (846) 335-18-36 www.ssau.ru, e-mail: ssau@ssau.ru

The objective function

$$J\left(\mathbf{M}_{X_1X_2}\right)=\sum_{i=1}^{n}\alpha_i\left(\mathbf{U}_1^i-\mathbf{M}_{X_1X_2}\cdot\mathbf{U}_2^i\right)^T\left(\mathbf{U}_1^i-\mathbf{M}_{X_1X_2}\cdot\mathbf{U}_2^i\right) \qquad (2.1)$$

where $\mathbf{M}_{X_1X_2}$ is the matrix describing the connection between the OFR and the BFR, parameterized by quaternions;

$\mathbf{U}_1^i, \mathbf{U}_2^i$ are the using vectors in the BFR and the OFR respectively;

n is the number of measuring vectors; min I = 2

α_i is the weight coefficient ($\alpha_i \neq 0$), considering the relative significance of measurements.

Four-dimensional symmetric matrix

$$\mathbf{B}=\sum_{i=1}^{n}\alpha_i\begin{bmatrix}\mathbf{I}\left(\left(\mathbf{U}_1^i\right)^T\mathbf{U}_2^i\right)-\mathbf{U}_2^i\left(\mathbf{U}_1^i\right)^T-\mathbf{U}_1^i\left(\mathbf{U}_2^i\right)^T & -\left(\mathbf{U}_1^i\times\mathbf{U}_2^i\right)\\ -\left(\mathbf{U}_1^i\times\mathbf{U}_2^i\right)^T & -\left(\mathbf{U}_1^i\right)^T\mathbf{U}_2^i\end{bmatrix}. \qquad (2.2)$$

2. Nanosatellite attitude determination algorithm on one-shot measurements (Wahba problem)

Example

Measurements

BFR

Earth magnetizing force

Current from solar battery panels

- measured Earth magnetic vector in the body frame of reference

- current in the body frame of reference

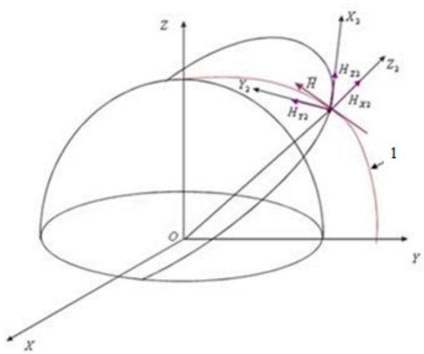

Algorithm QUEST

1 – power line of the Earth magnetic field;
2,3,4 – solar battery panels

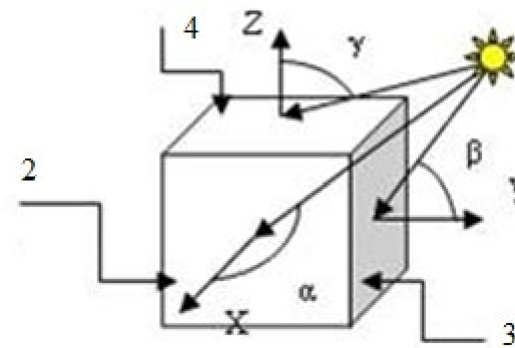

OFR

Model of the Earth magnetic field in the orbital frame of reference

Model of the Sun motion in the orbital frame of reference

Models

3.1 Linear problem. Basic concepts

Model	Continuous time	Discrete time
System	$\dot{\boldsymbol{x}}(t) = \boldsymbol{F}(t)\boldsymbol{x}(t) + \boldsymbol{\omega}(t)$	$\boldsymbol{x}_k = \boldsymbol{\Phi}_{k-1}\boldsymbol{x}_{k-1} + \boldsymbol{\omega}_k$
Measurements	$\boldsymbol{z} = \boldsymbol{H}(t)\boldsymbol{x}(t) + \boldsymbol{v}(t)$	$\boldsymbol{z}_k = \boldsymbol{H}_k\boldsymbol{x}_k + \boldsymbol{v}_k$
System noise	$E\langle \boldsymbol{\omega}(t) \rangle = 0$ $E\langle \boldsymbol{\omega}(t)\boldsymbol{\omega}^T(s) \rangle = \delta(t-s)\boldsymbol{Q}(t)$	$E\langle \boldsymbol{\omega}_k \rangle = 0$ $E\langle \boldsymbol{\omega}_k\boldsymbol{\omega}_i^T \rangle = \Delta(k-i)\boldsymbol{Q}_k$
Measurement noise	$E\langle \boldsymbol{v}(t) \rangle = 0$ $E\langle \boldsymbol{v}(t)\boldsymbol{v}^T(s) \rangle = \delta(t-s)\boldsymbol{R}(t)$	$E\langle \boldsymbol{v}_k \rangle = 0$ $E\langle \boldsymbol{v}_k\boldsymbol{v}_i^T \rangle = \Delta(k-i)\boldsymbol{R}_k$

3.1 Linear problem. Basic concepts

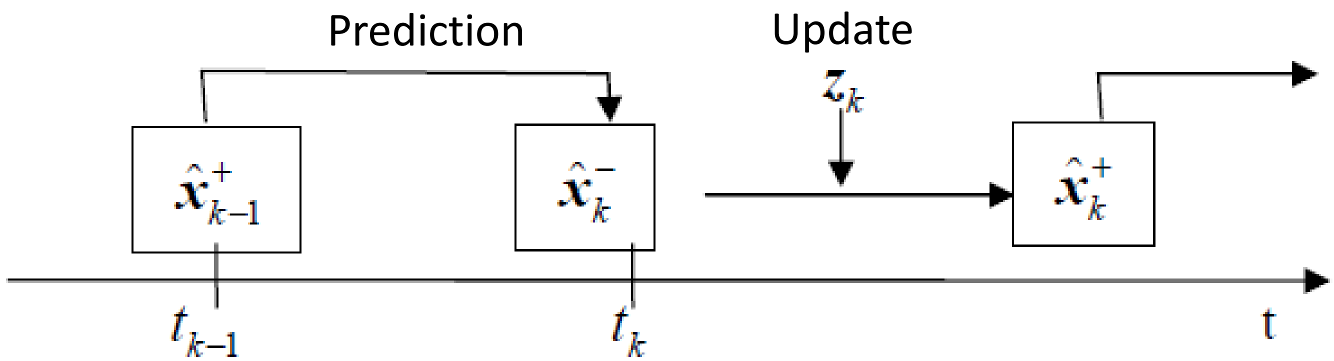

Fig. 3.1 - Kalman filter operation principle

The second moment of the random process can be described in terms of the covariance matrix

$$\boldsymbol{P}(t) = E\left\langle \left[\boldsymbol{x}(t) - \hat{\boldsymbol{x}}(t)\right]\left[\boldsymbol{x}(t) - \hat{\boldsymbol{x}}(t)\right]^{T} \right\rangle \qquad (3.1)$$

$$\dot{\boldsymbol{x}}(t) = \boldsymbol{F}(t)\boldsymbol{x}(t) \qquad \boldsymbol{x}(0) = \hat{\boldsymbol{x}}_{k-1}^{+}$$

Linear Models. Summary

Continuous linear process model and a discrete observation model:

$$\dot{\boldsymbol{x}}(t) = \boldsymbol{F}(t)\boldsymbol{x}(t) + \boldsymbol{\omega}(t)$$

$$\boldsymbol{z}_k = \boldsymbol{H}_k \boldsymbol{x}_k + \boldsymbol{\upsilon}_k .$$

The Kalman filter prediction equations:

$$\dot{\boldsymbol{x}}(t) = \boldsymbol{F}(t)\boldsymbol{x}(t)$$

$$\dot{\boldsymbol{P}}(t) = \boldsymbol{F}(t)\boldsymbol{P}(t) + \boldsymbol{P}(t)\boldsymbol{F}^T(t) + \boldsymbol{Q} .$$

The observational update equations:

$$\boldsymbol{K}_{\mathrm{k}}^1 = \boldsymbol{I} - \boldsymbol{K}_k \boldsymbol{H}_k ,$$

$$\overline{\boldsymbol{K}}_k = \boldsymbol{P}_k^- \boldsymbol{H}_k^T \left[\boldsymbol{H}_k \boldsymbol{P}_k^- \boldsymbol{H}_k^T + \boldsymbol{R}_k \right]^{-1} .$$

$$\hat{\boldsymbol{x}}_k^+ = \boldsymbol{K}_k^1 \hat{\boldsymbol{x}}_k^- + \overline{\boldsymbol{K}}_k \boldsymbol{z}_k .$$

$$\boldsymbol{P}_k^+ = (\boldsymbol{I} - \boldsymbol{K}_k \boldsymbol{H}_k)\boldsymbol{P}_k^- .$$

3.4. Kalman filter for nonlinear systems (the expanded filter)

We will assume that the continuous or discrete stochastic system can be presented by the nonlinear dynamic equation and the model equation describing measurements

Model	Continuous time	Discrete time
System	$\dot{\boldsymbol{x}}(t) = \boldsymbol{f}(\boldsymbol{x}(t), t) + \boldsymbol{\omega}(t)$	$\boldsymbol{x}_k = \boldsymbol{f}(\boldsymbol{x}_{k-1}, k-1) + \boldsymbol{\omega}_{k-1}$
Measurements	$\boldsymbol{z}(t) = \boldsymbol{h}(\boldsymbol{x}(t), t) + \boldsymbol{v}(t)$	$\boldsymbol{z}_k = \boldsymbol{h}(\boldsymbol{x}_k, k) + \boldsymbol{v}_k$

The applied method of linearization demands that functions **f** and **h** were twice continuously differentiable. We will designate a symbol **δ** the small deviation from the estimated trajectory:

$$\delta \boldsymbol{x}_k = \boldsymbol{x}_k - \hat{\boldsymbol{x}}_k^-,$$

$$\delta \boldsymbol{z}_k = \boldsymbol{z}_k - \boldsymbol{h}\left(\hat{\boldsymbol{x}}_k^-, k\right),$$

1. ***Problem of setting the initial approximations of attitude parameters***.
For effective operation of the filter it is necessary to have rather good initial state vector. For certain initial conditions the filter can not converge.
2. ***Linearization problem.*** Kalman filter for the work uses the linearized motion model. In case of rather slow motion (or in case of rather frequent measurements) the filter gives a satisfactory estimation of the state vector. Otherwise the filter will give the constant and growing error in the state vector estimation.
3. ***Setting problem***. The filter uses in the work the covariance matrices of errors which setting strongly influences the main characteristics of the filter: the convergence speed and the estimated state vector error after convergence.

4 Research of attitude determination algorithms for microsatellites of the 'Tabletsat' series

(Source: Ivanov D. S., Ivlev N. A., Karpenko S.O., Ovchinnikov M. Y. Attitude determination algorithms investigation for microsatellites of 'TabletSat' series)

4.1 Characteristics of measuring data

Table 5.1

Characteristic	Magnetometer (MAG)	Sun sensor (SS)	Angular rate sensor (GYR)	Star tracker (ST)
Measurement range	±200 000 ntesla	±45 deg	±250 deg/c	±2 deg
Random deviation (σ)	250 ntesla	0,1 deg	0,005 deg/c	0,001 deg

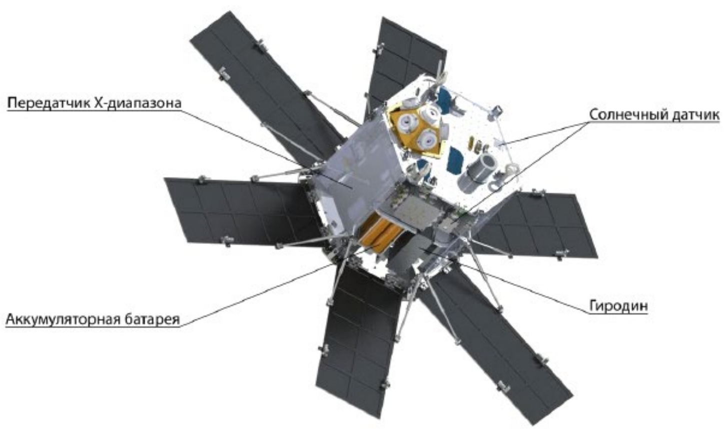

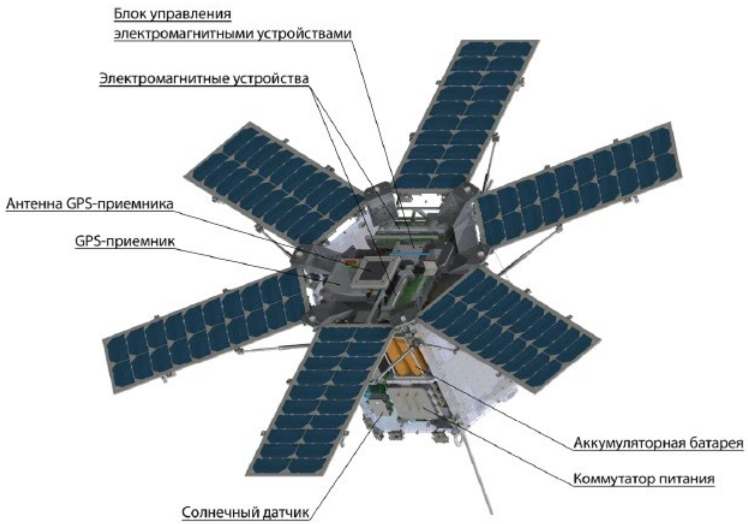

Moskovskoye shosse, 34, Samara, 443086, Russia, tel.: +7 (846) 335-18-26, fax: +7 (846) 335-18-36, www.ssau.ru, e-mail: ssau@ssau.ru

4.2 Creation of algorithms
4.2.1 Expanded Kalman filter

The Kalman filter

$$\dot{\mathbf{x}}(t) = \mathbf{f}(\mathbf{x}, t) + \mathbf{w}(t), \quad (4.1)$$

$$\mathbf{z}(t) = \mathbf{h}(\mathbf{x}, t) + \mathbf{v}(t). \quad (4.2)$$

The matrix of system dynamics and matrix of measurement model are calculated as follows:

$$H_k = \left.\frac{\partial \mathbf{h}(\mathbf{x}, t)}{\partial \mathbf{x}}\right|_{\mathbf{x}=\hat{\mathbf{x}}_k^-, t=t_k}, \quad F_k = \left.\frac{\partial \mathbf{f}(\mathbf{x}, t)}{\partial \mathbf{x}}\right|_{\mathbf{x}=\hat{\mathbf{x}}_k^-, t=t_k}. \quad (4.3)$$

The prediction stage:

$$\hat{\mathbf{x}}_k^- = \int_{t_{k-1}}^{t_k} \mathbf{f}(\hat{\mathbf{x}}_{k-1}^+, t)dt, \quad (4.4)$$

$$P_k^- = \Phi_k P_{k-1}^+ \Phi_k^{\mathrm{T}} + Q_k.$$

The update stage:

$$K_k = P_k^- H_k^{\mathrm{T}} (H_k P_k^- H_k^{\mathrm{T}} + R_k)^{-1},$$

$$\hat{\mathbf{x}}_k^+ = \hat{\mathbf{x}}_k^- + K_k[\mathbf{z}_k - \mathbf{h}(\hat{\mathbf{x}}_k^-, t_k)], \quad (4.5)$$

$$P_k^+ = [E - K_k H_k] P_k^-.$$

Numerical simulations:

1. ST+GYR+MAG+SS
2. ST+GYR+MAG
3. ST+MAG+SS
4. ST+MAG
5. MAG+SS+GYR
6. ST+GYR
7. MAG+SS
8. MAG+GYR
9. ST

Moskovskoye shosse, 34, Samara, 443086, Russia, tel.: +7 (846) 335-18-26, fax: +7 (846) 335-18-36, www.ssau.ru, e-mail: ssau@ssau.ru

4.2.3. Filtration with calibration

We will consider the following model of measurement of the sensor of angular rate:

$$\tilde{\boldsymbol{\omega}} = \boldsymbol{\omega} + \Delta\boldsymbol{\omega} + \boldsymbol{\eta}_{\omega}, \qquad (4.8)$$

$$\Delta\dot{\boldsymbol{\omega}} = \boldsymbol{\eta}_{\Delta\omega}.$$

We will similarly use the following model of measurements of the magnetometer:

$$\tilde{\mathbf{b}} = A(\boldsymbol{\lambda}_k^-)\mathbf{b}_o + \Delta\mathbf{b} + \boldsymbol{\eta}_{\mathrm{b}},$$

$$\Delta\dot{\mathbf{b}} = \boldsymbol{\eta}_{\Delta\mathrm{b}},$$

Table 5.2. The sensitivity matrices for various sets of sensors

Sensors	Measurement vector	State vector	Measurement matrix *H*	Accuracy (deg; deg/s)
1. ST+GYR+MAG+SS	$\begin{pmatrix} \boldsymbol{\lambda} \\ \boldsymbol{\omega} \\ \mathbf{b} \\ \mathbf{s} \end{pmatrix}$	$\begin{pmatrix} \boldsymbol{\lambda} \\ \boldsymbol{\omega} \end{pmatrix}$	$\begin{pmatrix} E_{3\times3} & 0_{3\times3} \\ 0_{3\times3} & E_{3\times3} \\ W_{\hat{\mathbf{b}}} & 0_{3\times3} \\ W_{\hat{\mathbf{s}}} & 0_{3\times3} \end{pmatrix}$	$5\cdot10^{-4}$ $4\cdot10^{-4}$

Table 4.2. Continuation

Sensors	Measurement vector	State vector	Measurement matrix *H*	Accuracy (deg; deg/s)
2. ST+GYR+MAG	$\begin{pmatrix} \boldsymbol{\lambda} \\ \boldsymbol{\omega} \\ \mathbf{b} \end{pmatrix}$	$\begin{pmatrix} \boldsymbol{\lambda} \\ \boldsymbol{\omega} \end{pmatrix}$	$\begin{pmatrix} E_{3\times3} & 0_{3\times3} \\ 0_{3\times3} & E_{3\times3} \\ W_{\hat{\mathbf{b}}} & 0_{3\times3} \end{pmatrix}$	$5\cdot10^{-4}$; $4\cdot10^{-4}$
3. ST+MAG+SS	$\begin{pmatrix} \boldsymbol{\lambda} \\ \mathbf{b} \\ \mathbf{s} \end{pmatrix}$	$\begin{pmatrix} \boldsymbol{\lambda} \\ \boldsymbol{\omega} \end{pmatrix}$	$\begin{pmatrix} E_{3\times3} & 0_{3\times3} \\ W_{\hat{\mathbf{b}}} & 0_{3\times3} \\ W_{\hat{\mathbf{s}}} & 0_{3\times3} \end{pmatrix}$	$7\cdot10^{-4}$; $6\cdot10^{-4}$
4. ST+MAG	$\begin{pmatrix} \boldsymbol{\lambda} \\ \mathbf{b} \end{pmatrix}$	$\begin{pmatrix} \boldsymbol{\lambda} \\ \boldsymbol{\omega} \\ \Delta\mathbf{b} \end{pmatrix}$	$\begin{pmatrix} E_{3\times3} & 0_{3\times3} & 0_{3\times3} \\ W_{\hat{\mathbf{b}}} & 0_{3\times3} & E_{3\times3} \end{pmatrix}$	$7\cdot10^{-4}$ $6\cdot10^{-4}$

Table 4.2. Continuation

Sensors	Measurement vector	State vector	Measurement matrix H	Accuracy (deg; deg/s)
5. MAG+SS+GYR	$\begin{pmatrix} \mathbf{b} \\ \mathbf{s} \\ \boldsymbol{\omega} \end{pmatrix}$	$\begin{pmatrix} \boldsymbol{\lambda} \\ \boldsymbol{\omega} \end{pmatrix}$	$\begin{pmatrix} W_{\hat{\mathbf{b}}} & 0_{3\times3} \\ W_{\hat{\mathbf{s}}} & 0_{3\times3} \\ 0_{3\times3} & E_{3\times3} \end{pmatrix}$	$2\cdot10^{-2}$ $4\cdot10^{-3}$
		$\begin{pmatrix} \boldsymbol{\lambda} \\ \boldsymbol{\omega} \\ \Delta\boldsymbol{\omega} \end{pmatrix}$	$\begin{pmatrix} W_{\hat{\mathbf{b}}} & 0_{3\times3} & 0_{3\times3} \\ W_{\hat{\mathbf{s}}} & 0_{3\times3} & 0_{3\times3} \\ 0_{3\times3} & E_{3\times3} & E_{3\times3} \end{pmatrix}$	$2\cdot10^{-2}$ $4\cdot10^{-3}$
		$\begin{pmatrix} \boldsymbol{\lambda} \\ \boldsymbol{\omega} \\ \Delta\mathbf{b} \end{pmatrix}$	$\begin{pmatrix} W_{\hat{\mathbf{b}}} & 0_{3\times3} & E_{3\times3} \\ W_{\hat{\mathbf{s}}} & 0_{3\times3} & 0_{3\times3} \\ 0_{3\times3} & E_{3\times3} & 0_{3\times3} \end{pmatrix}$	$5\cdot10^{-2}$ $4\cdot10^{-3}$

Moskovskoye shosse, 34, Samara, 443086, Russia, tel.: +7 (846) 335-18-26, fax: +7 (846) 335-18-36, www.ssau.ru, e-mail: ssau@ssau.ru

Table 4.2. Continuation

Sensors	Measurement vector	State vector	Measurement matrix *H*	Accuracy (deg; deg/s)
6. ST+GYR	$\begin{pmatrix}\boldsymbol{\lambda}\\ \boldsymbol{\omega}\end{pmatrix}$	$\begin{pmatrix}\boldsymbol{\lambda}\\ \boldsymbol{\omega}\end{pmatrix}$	$\begin{pmatrix}E_{3\times3} & 0_{3\times3}\\ 0_{3\times3} & E_{3\times3}\end{pmatrix}$	$5\cdot10^{-4}$ $4\cdot10^{-4}$
		$\begin{pmatrix}\boldsymbol{\lambda}\\ \boldsymbol{\omega}\\ \Delta\boldsymbol{\omega}\end{pmatrix}$	$\begin{pmatrix}E_{3\times3} & 0_{3\times3} & 0_{3\times3}\\ 0_{3\times3} & E_{3\times3} & E_{3\times3}\end{pmatrix}$	$5\cdot10^{-4}$ $4\cdot10^{-4}$
7. MAG+SS	$\begin{pmatrix}\mathbf{b}\\ \mathbf{s}\end{pmatrix}$	$\begin{pmatrix}\boldsymbol{\lambda}\\ \boldsymbol{\omega}\end{pmatrix}$	$\begin{pmatrix}W_{\hat{\mathbf{b}}} & 0_{3\times3}\\ W_{\hat{\mathbf{s}}} & 0_{3\times3}\end{pmatrix}$	$1{,}2\cdot10^{-1}$ $2\cdot10^{-2}$
8. MAG+GYR	$\begin{pmatrix}\mathbf{b}\\ \boldsymbol{\omega}\end{pmatrix}$	$\begin{pmatrix}\boldsymbol{\lambda}\\ \boldsymbol{\omega}\end{pmatrix}$	$\begin{pmatrix}W_{\hat{\mathbf{b}}} & 0_{3\times3}\\ 0_{3\times3} & E_{3\times3}\end{pmatrix}$	$2\cdot10^{-1}$ $5\cdot10^{-3}$
9. ST	$\boldsymbol{\lambda}$	$\begin{pmatrix}\boldsymbol{\lambda}\\ \boldsymbol{\omega}\end{pmatrix}$	$E_{3\times3}$	$8\cdot10^{-4}$ $6\cdot10^{-4}$

Numerical simulations:

1. ST+GYR+MAG+SS
2. ST+GYR+MAG
3. ST+MAG+SS
4. ST+MAG
5. MAG+SS+GYR
6. ST+GYR
7. MAG+SS
8. MAG+GYR
9. ST

1–4, 6, 9: (~10^{-4} deg; ~10^{-4} deg/s)

5: (~10^{-2} deg; ~10^{-3} deg/s)

7: (~10^{-1} deg; ~10^{-2} deg/s)

8: (~10^{-1} deg; ~10^{-3} deg/s)

4.3 Research of angular motion determination algorithms

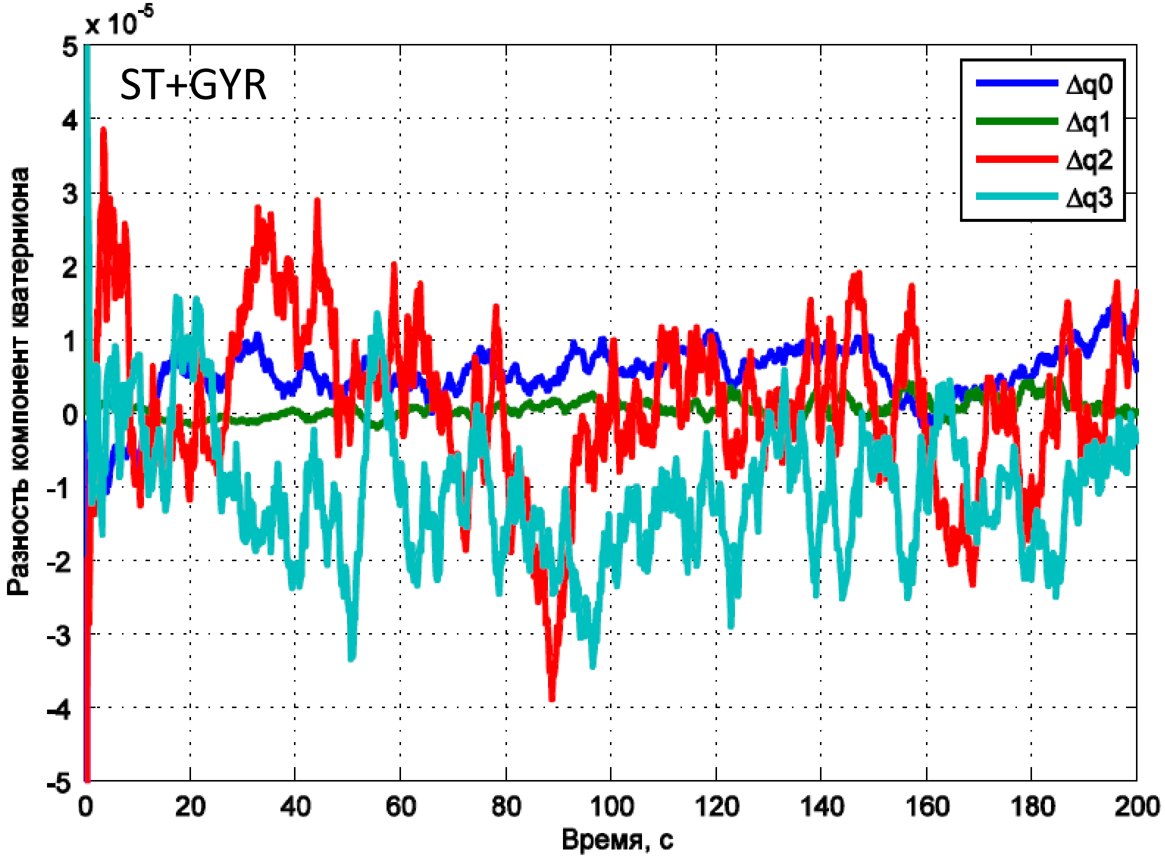

Fig. 4.1 - The graph of the difference of quaternion component estimates and their real value

Moskovskoye shosse, 34, Samara, 443086, Russia, tel.: +7 (846) 335-18-26, fax: +7 (846) 335-18-36, www.ssau.ru, e-mail: ssau@ssau.ru

4.3 Research of angular motion determination algorithms

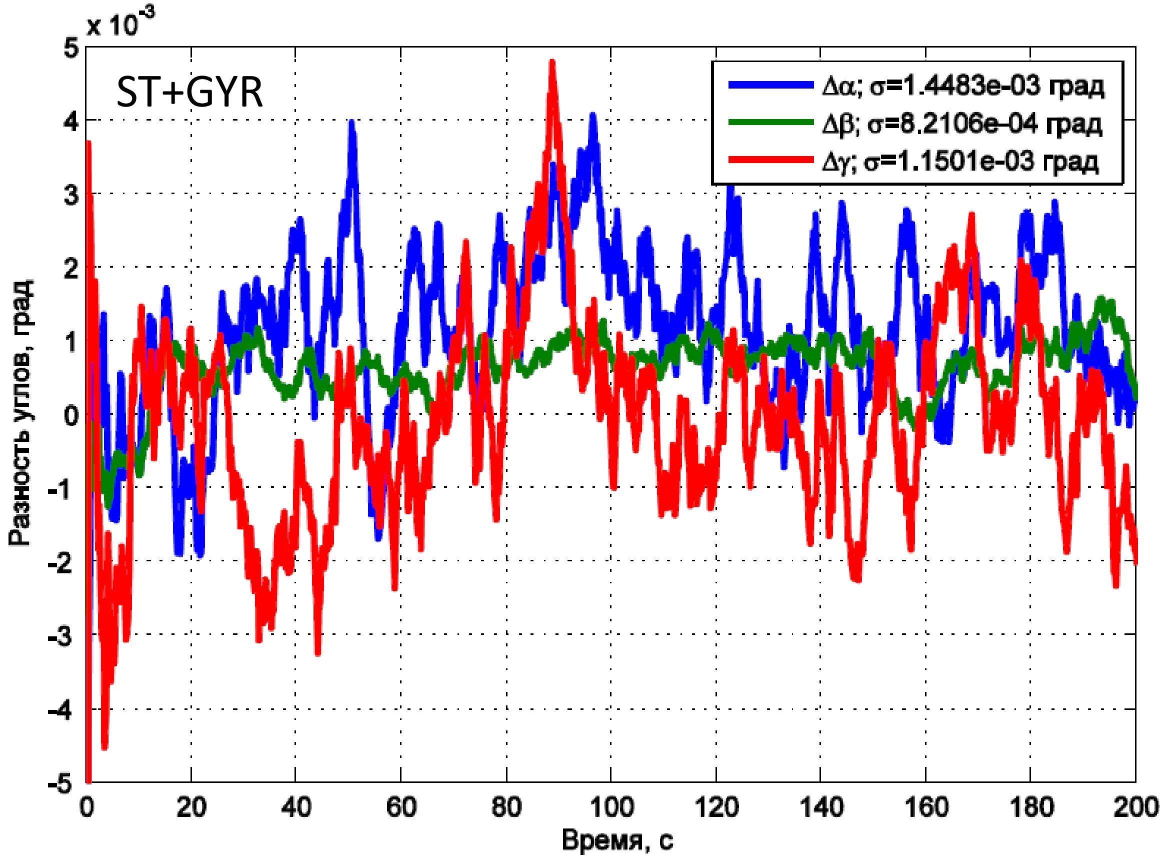

Fig. 4.2 - The graph of the difference of estimates of attitude angles and their real value

4.3 Research of angular motion determination algorithms

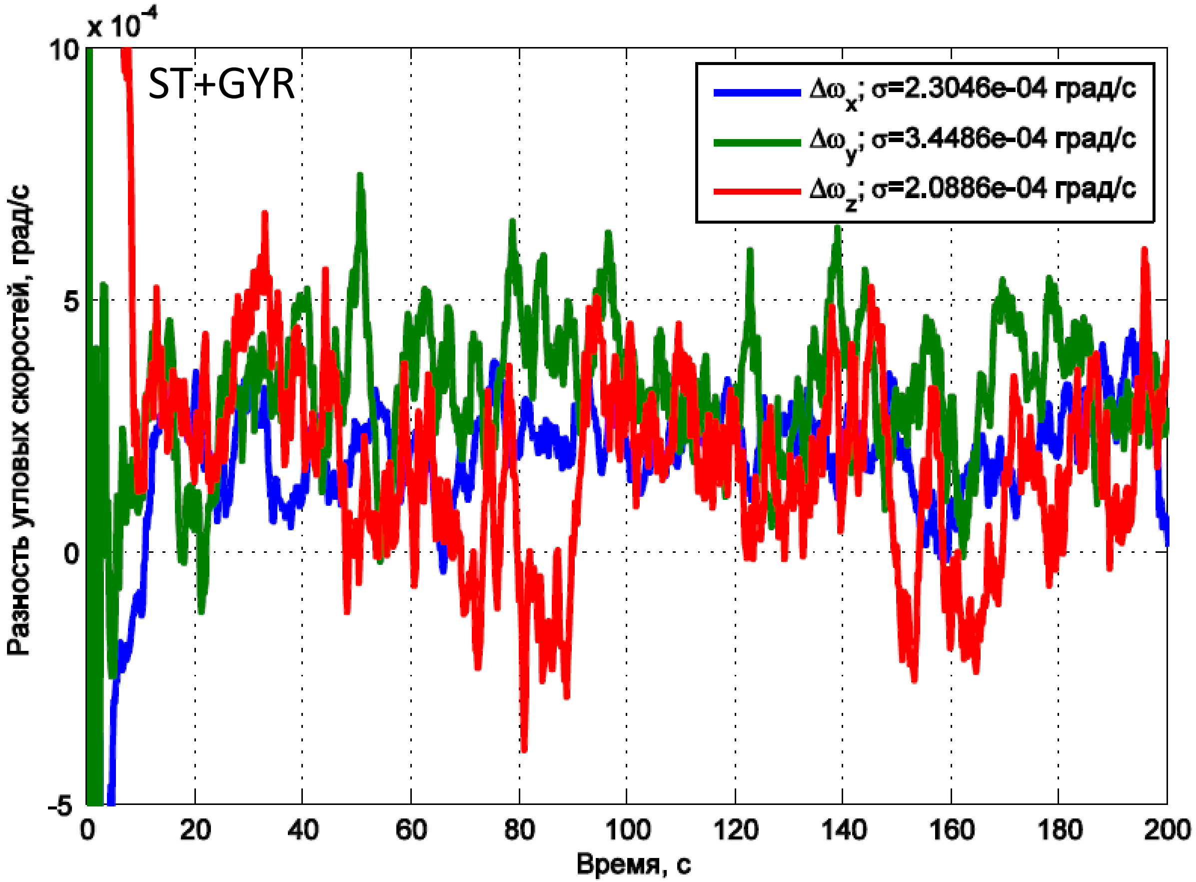

Fig 4.3 - - The graph of the difference of angular rate component estimates and their real value

Moskovskoye shosse, 34, Samara, 443086, Russia, tel.: +7 (846) 335-18-26, fax: +7 (846) 335-18-36, www.ssau.ru, e-mail: ssau@ssau.ru

4.3 Research of angular motion determination algorithms

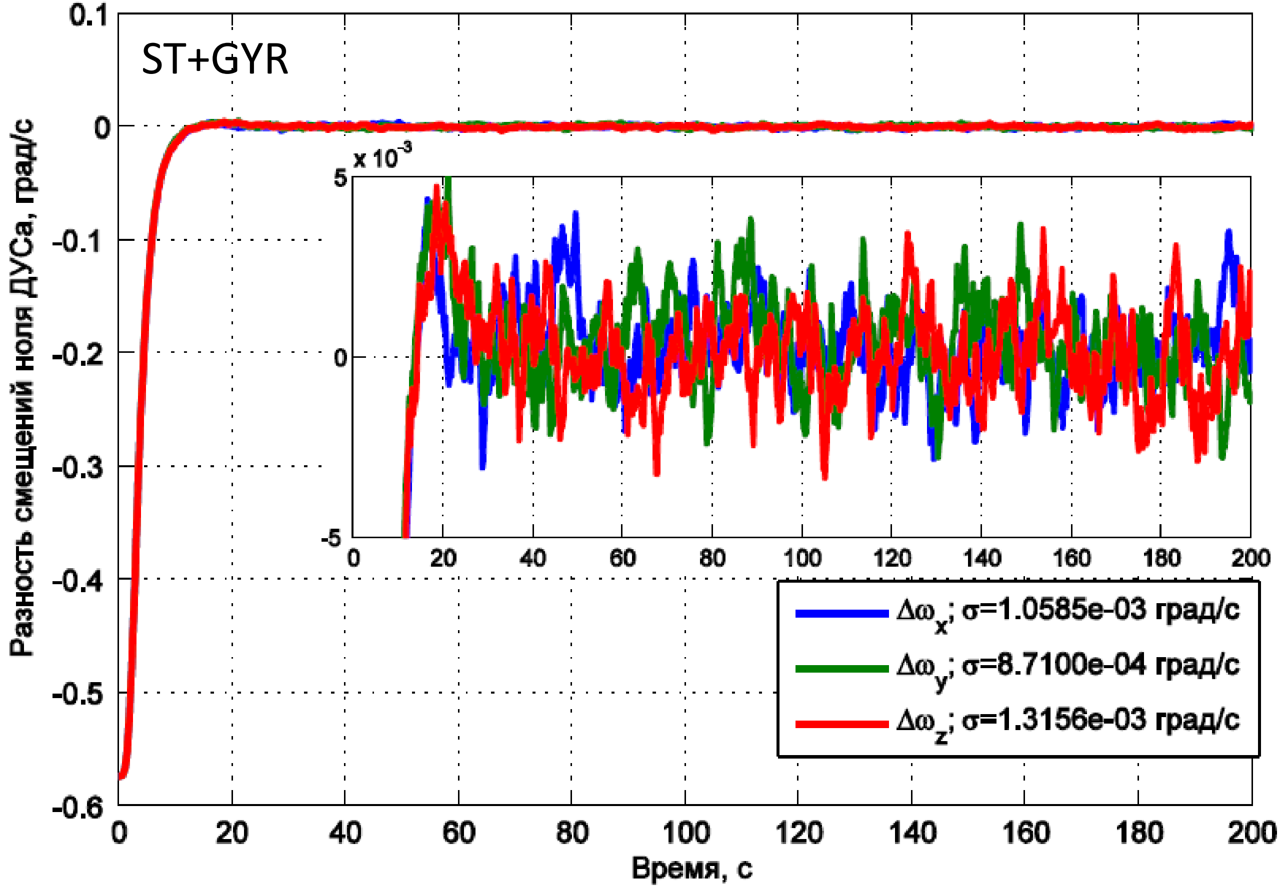

Fig. 4.4 - The graph of the difference of estimates component of shift of zero of sensor of angular rate and their real value

5.3 Research of angular motion determination algorithms

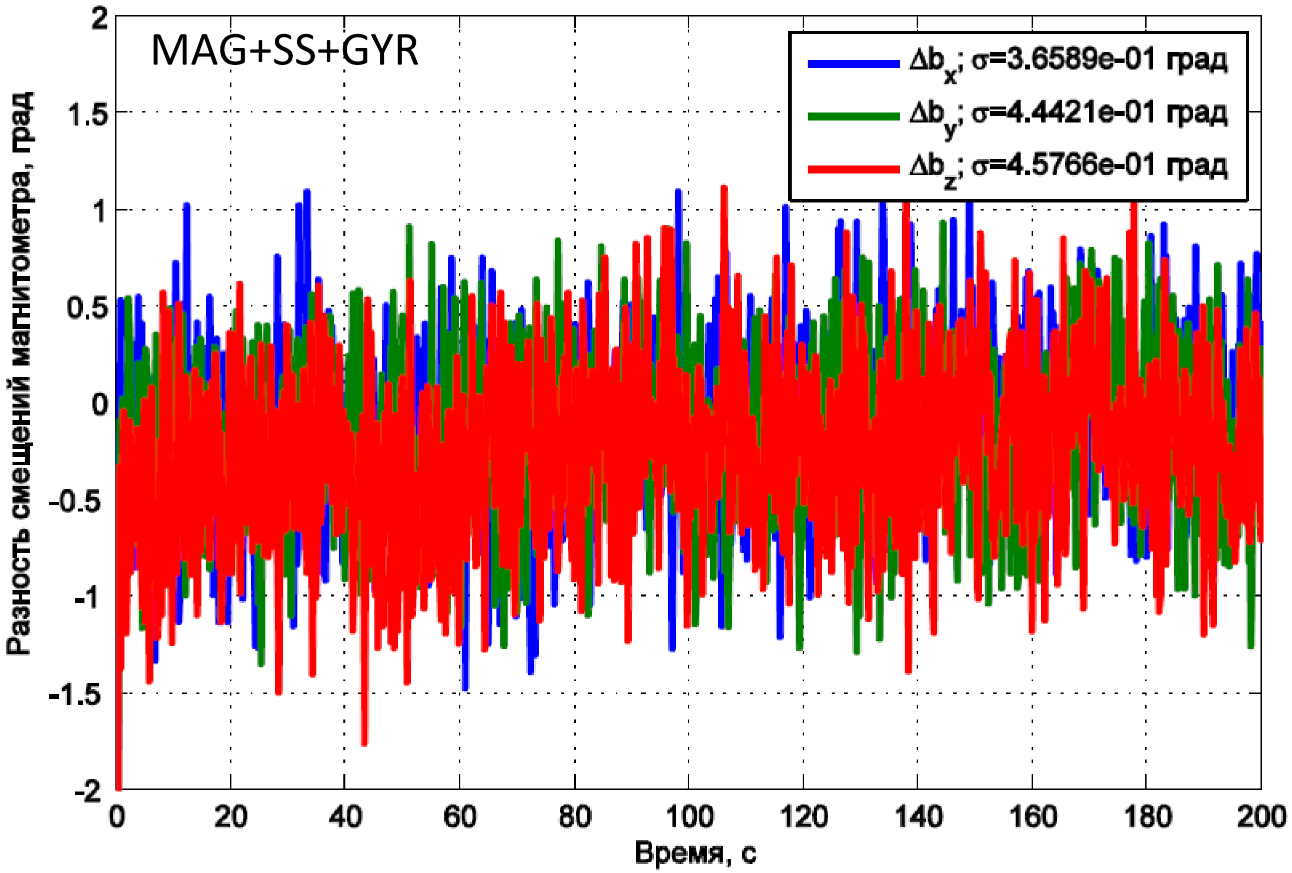

Fig. 4.5 - The graph of the difference of estimates component of shift of zero of magnetometer and their real value

САМАРСКИЙ УНИВЕРСИТЕТ
SAMARA UNIVERSITY

THANK YOU

34, Moskovskoye shosse, Samara, 443086, Russia
Tel.: +7 (846) 335-18-26, fax: +7 (846) 335-18-36
www.ssau.ru, e-mail: ssau@ssau.ru

3.1 Linear problem. Basic concepts

Let's consider the system

$$\dot{\boldsymbol{x}}(t) = \boldsymbol{F}(t)\boldsymbol{x}(t) + \boldsymbol{\omega}(t) \qquad (3.2)$$

The solution (3.2) with the initial condition $\boldsymbol{x}(t_0)$ and the transfer state matrix $\boldsymbol{\Phi}(t,t_0)$ is

$$\boldsymbol{x}(t) = \boldsymbol{\Phi}(t,t_0)\boldsymbol{x}(t_0) + \int_{t_0}^{t} \boldsymbol{\Phi}(t,\tau)\boldsymbol{\omega}(\tau)d\tau .$$

The mean value of this value is

$$\mathrm{E}\langle \boldsymbol{x}(t)\rangle = \boldsymbol{\Phi}(t,t_0)\mathrm{E}\langle \boldsymbol{x}(t_0)\rangle + \int_{t_0}^{t} \boldsymbol{\Phi}(t,\tau)\langle \boldsymbol{\omega}(\tau)\rangle d\tau .$$

Then

$$\left[\boldsymbol{x}(t) - \mathrm{E}\langle \boldsymbol{x}(t)\rangle\right] = \boldsymbol{\Phi}(t,t_0)\left[\boldsymbol{x}(t_0) - \mathrm{E}\langle \boldsymbol{x}(t_0)\rangle\right] + \int_{t_0}^{t} \boldsymbol{\Phi}(t,\tau)\boldsymbol{\omega}(\tau)d\tau . \qquad (3.3)$$

Substituting (3.3) in (3.1), making some transformations and calculating the first derivative of the P(t) function, as a result we will receive

$$\dot{\boldsymbol{P}}(t) = \boldsymbol{F}(t)\boldsymbol{P}(t) + \boldsymbol{P}(t)\boldsymbol{F}^{T}(t) + \boldsymbol{Q} . \qquad (3.4)$$

$$\boldsymbol{P}(0) = \boldsymbol{P}_{k\text{-}1}^{+}$$

3.2. The feedback coupling coefficient matrix

Measurements linearly depend on the state vector and are described by the equation

$$z_k = H_k x_k + v_k . \tag{3.5}$$

$$\hat{x}_k^+ = K_k^1 \hat{x}_k^- + \bar{K}_k z_k . \tag{3.6}$$

The matrices K_k^1 и $\bar{K}_k$ let's find from the condition

$$\begin{gathered} \mathrm{E}\left\langle \left[x_k - \hat{x}_k^+ \right] z_i^T \right\rangle = 0, i = 1, 2, \ldots, k-1, \\ \mathrm{E}\left\langle \left[x_k - \hat{x}_k^+ \right] z_k^T \right\rangle = 0 . \end{gathered} \tag{3.7}$$

Substituting (3.1) and (3.6) in the equation (3.7)

$$K_k^1 = I - K_k H_k , \tag{3.8}$$

$$\bar{K}_k = P_k^- H_k^T \left[H_k P_k^- H_k^T + R_k \right]^{-1} . \tag{3.9}$$

This matrix of coefficients is the function from a priori value of the error covariance matrix.

3.3. The correction of the value of the covariance matrix of error of state vector estimation

By definition the posteriori covariance matrix of error is written as follows

$$P_k(+) = E\left\langle \tilde{x}_k^+ \tilde{x}_k^{+T} \right\rangle, \qquad (3.10)$$

where

$$\tilde{x}_k^+ = \hat{x}_k^+ - x_k, \; \tilde{x}_k^- = \hat{x}_k^- - x_k. \qquad (3.11)$$

Substituting (3.8) in (3.6), we will receive

$$\hat{x}_k^+ = \hat{x}_k^- + \bar{K}_k\left[z_k - H_k \hat{x}_k^-\right]. \qquad (3.12)$$

We will subtract x_k from both parts (3.12) and we will substitute in it $\boldsymbol{z}_k$ value according to the equation (3.5). As a result we will receive

$$\hat{x}_k^+ - x_k = \hat{x}_k^- + \bar{K}_k H_k x_k + \bar{K}_k v_k - \bar{K}_k H_k \hat{x}_k^- - x_k$$

or taking into account (3.11) we will receive

$$\tilde{x}_k^+ = \left(I - \bar{K}_k H_k\right)\tilde{x}_k^- + \bar{K}_k v_k. \qquad (3.13)$$

Substituting (3.13) in (3.10) and in view of $E\left\langle \tilde{x}_k^- v_k^T \right\rangle = 0$ we will receive

$$P_k^+ = (I - K_k H_k) P_k^-. \qquad (3.14)$$

Then *f(**x**, k-1)* at a point $\boldsymbol{x} = \hat{\boldsymbol{x}}_{k-1}^{-}$ can be presented in the form

$$\boldsymbol{x}_k = \boldsymbol{f}(\boldsymbol{x}_{k-1}, k-1) = \boldsymbol{x}_k^{-} + \left.\frac{\partial \boldsymbol{f}(\boldsymbol{x}, k-1)}{\partial \boldsymbol{x}}\right|_{\boldsymbol{x}=\hat{\boldsymbol{x}}_{k-1}^{-}} \delta \boldsymbol{x}_{k-1}.$$

Thus, we receive

$$\delta \boldsymbol{x}_k \approx \boldsymbol{\Phi}_{k-1}^{[1]} \delta \boldsymbol{x}_{k-1} + \boldsymbol{\omega}_{k-1},$$

where

$$\boldsymbol{\Phi}_{k-1}^{[1]} = \left.\frac{\partial \boldsymbol{f}(\boldsymbol{x}, k-1)}{\partial \boldsymbol{x}}\right|_{\boldsymbol{x}=\hat{\boldsymbol{x}}_{k-1}^{-}} \delta \boldsymbol{x}_{k-1}. \quad (3.15)$$

In turn, measurements can be presented in the decomposition form in a row of Taylor at a point $\boldsymbol{x} = \hat{\boldsymbol{x}}_k^{-}$ as follows

$$\boldsymbol{h}(\boldsymbol{x}, k) = \boldsymbol{h}(\hat{\boldsymbol{x}}_k^{-}, k) + \left.\frac{\partial \boldsymbol{h}(\boldsymbol{x}, k)}{\partial \boldsymbol{x}}\right|_{\boldsymbol{x}=\hat{\boldsymbol{x}}_k^{-}} \delta \boldsymbol{x}_k \text{ и } \delta \boldsymbol{z}_k = \left.\frac{\partial \boldsymbol{h}(\boldsymbol{x}, k)}{\partial \boldsymbol{x}}\right|_{\boldsymbol{x}=\hat{\boldsymbol{x}}_k^{-}} \delta \boldsymbol{x}_k.$$

The additive components above the first order are left out here. If in decomposition we neglect members of a high order, then disturbance $\boldsymbol{z}_k$ can be presented in the form

$$\delta \boldsymbol{z}_k = \boldsymbol{H}_k^{[1]} \delta \boldsymbol{x}_k,$$

where

$$\boldsymbol{H}_k^{[1]} = \left.\frac{\partial \boldsymbol{h}(\boldsymbol{x}, k)}{\partial \boldsymbol{x}}\right|_{\boldsymbol{x}=\hat{\boldsymbol{x}}_k^{-}}. \quad (3.16)$$

4.2 Creation of algorithms

4.2.2. The motion model and measurement model

We will accept that the dynamic model of the microsatellite motion used by Kalman filter considers only the gravitational and control torques from flywheels and is

$$J\dot{\boldsymbol{\omega}} = -\dot{\mathbf{h}} + \frac{3\mu}{r^3}(\boldsymbol{\eta} \times J\boldsymbol{\eta}) - \boldsymbol{\omega} \times (J\boldsymbol{\omega} + \mathbf{k}), \qquad (4.6)$$

Change of the kinetic torque of flywheels which is set by expression

$$\dot{\mathbf{k}} = K_{\alpha}\boldsymbol{\lambda}_{rel} + K_{\omega}(\tilde{\boldsymbol{\omega}} - \tilde{\boldsymbol{\omega}}_0) - \boldsymbol{\omega} \times (J\boldsymbol{\omega} + \mathbf{k}),$$

Kinematic equations

$$\dot{\Lambda} = \frac{1}{2}\Omega\Lambda. \qquad (4.7)$$

Here

$$\Omega = \begin{pmatrix} \tilde{W} & \tilde{\boldsymbol{\omega}} \\ -\tilde{\boldsymbol{\omega}}^T & 0 \end{pmatrix},$$

Moskovskoye shosse, 34, Samara, 443086, Russia, tel.: +7 (846) 335-18-26, fax: +7 (846) 335-18-36, www.ssau.ru, e-mail: ssau@ssau.ru

Let's write equations (5.6) and (5.7) as follows

$$\frac{d}{dt}\delta\mathbf{x}(t) = F(t)\delta\mathbf{x}(t),$$

The linearized motion equation matrix at a point of state

$$F = \begin{pmatrix} -W_\omega & \frac{1}{2}E \\ J^{-1}\left(kF_g - K_\alpha W_{\Lambda_{rel}}\right) & -J^{-1}K_\omega \end{pmatrix},$$

$$W_{\Lambda_{rel}} = \begin{pmatrix} \lambda_{rel}^0 & -\lambda_{rel}^3 & \lambda_{rel}^2 \\ \lambda_{rel}^3 & \lambda_{rel}^0 & -\lambda_{rel}^1 \\ -\lambda_{rel}^2 & \lambda_{rel}^1 & \lambda_{rel}^0 \end{pmatrix},$$

For various set of measuring sensors the filtering algorithms will differ in the measurement model (5.2) linearized by the measurement matrix H (5.3). These values are given in table 5.2. Values of the measurement error matrx R have the diagonal appearance for all sets of sensors. On the diagonal of the matrix there are dispersions of errors of the corresponding sensors which characteristics are provided in table 5.1.

For example, for the filter using measurements of the magnetometer and the solar vector, the measurement vector consists of the vector of the geomagnetic field b and the hector of the direction to the Sun of s. Then h vector from (5.2) can be written as follows

$$\mathbf{h} = \left[\left(A(\hat{\Lambda}_k^-)\mathbf{b}_o \right)^T \quad \left(A(\hat{\Lambda}_k^-)\mathbf{s}_o \right)^T \right]^T,$$

The linearized measurement model is written as follows:

$$\delta \mathbf{z}(t) = H(t)\delta \mathbf{x}(t).$$

Here δz(t) is the small change of measurements at small change of the state vector δx(t) in the moment of time t.

The matrix of sensitivity of H has an appearance

$$H = \begin{pmatrix} W_{\hat{\mathbf{b}}} & 0_{3\times3} \\ W_{\hat{\mathbf{s}}} & 0_{3\times3} \end{pmatrix},$$

Where $W_{\hat{\mathbf{b}}}$, $W_{\hat{\mathbf{s}}}$ are the skew-symmetric matrices of the measurement predition $\hat{\mathbf{b}} = A(\hat{\Lambda}_k^-)\mathbf{b}_o$ $\hat{\mathbf{s}} = A(\hat{\Lambda}_k^-)\hat{\mathbf{s}}_o$ respectively.